

Simplifying the Complex ^1H NMR Spectra of Fluorine-Substituted Benzamides by Spin System Filtering and Spin-State Selection: Multiple-Quantum–Single-Quantum Correlation

Bikash Baishya,^{†,‡} G. N. Manjunatha Reddy,[‡] Uday Ramesh Prabhu,^{†,‡} T. N. Guru Row,[†] and N. Suryaprakash^{*,‡}

Solid State and Structural Chemistry Unit and NMR Research Centre, Indian Institute of Science, Bangalore 560 012, India

Received: June 23, 2008; Revised Manuscript Received: August 9, 2008

The proton NMR spectra of fluorine-substituted benzamides are very complex (Figure 1) due to severe overlap of ^1H resonances from the two aromatic rings, in addition to several short and long-range scalar couplings experienced by each proton. With no detectable scalar couplings between the inter-ring spins, the ^1H NMR spectra can be construed as an overlap of spectra from two independent phenyl rings. In the present study we demonstrate that it is possible to separate the individual spectrum for each aromatic ring by spin system filtering employing the multiple-quantum–single-quantum correlation methodology. Furthermore, the two spin states of fluorine are utilized to simplify the spectrum corresponding to each phenyl ring by the spin-state selection. The demonstrated technique reduces spectral complexity by a factor of 4, in addition to permitting the determination of long-range couplings of less than 0.2 Hz and the relative signs of heteronuclear couplings. The technique also aids the judicious choice of the spin-selective double-quantum–single-quantum J -resolved experiment to determine the long-range homonuclear couplings of smaller magnitudes.

1. Introduction

NMR spectroscopy is a powerful technique for the investigation of molecular structure, conformation, and dynamics. The line positions and the line intensities in the high-resolution single-quantum (SQ) NMR spectra of diamagnetic materials in the solution state depend on the chemical shifts (δ_i) and the scalar couplings (J_{ij}). The information on the molecular structure and conformation is obtained using these parameters, particularly the three-bond J_{ij} values for obtaining the dihedral angle restraints.^{1–3} In a weakly coupled spin system, the first-order analysis of the spectrum is straightforward. For the measurement of scalar couplings in such systems several two-dimensional methodologies are available in the literature, viz., COSY,^{4,5} J -resolved,^{6–12} and quantitative J correlation experiments.^{13–15} In systems with limited complexity, a single COSY spectrum allows the identification of a coupled spin network and also the accurate measurement of all the coupling constants. As far as the determination of the relative signs and magnitudes of the coupling constants is concerned, in larger or complex spin systems often COSY spectra alone are not sufficient for the analyses. The problem in such situations is the overlap of numerous multiplet components arising from too many couplings of different magnitudes. Hence, several strategies have been developed over the years to reduce the number of peaks in the multiplet pattern, viz., Z-COSY,¹⁶ soft-COSY,¹⁷ and E-COSY.^{18–25}

Recently we have demonstrated that, in aromatic systems such as 2-fluoropyridine, 1-chloro-2-fluorobenzene where each proton experiences several long- and short-range scalar couplings, the spin-selective multiple-quantum (MQ)–SQ correlation experiment results in drastic simplification of complex ^1H spectra.^{26,27}

In the present study we demonstrate the analyses of complex ^1H NMR spectra of 3-fluoro-*N*-(3-fluorophenyl)benzamide (**1**) and 3-fluoro-*N*-(4-fluorophenyl)benzamide (**2**) shown in Figure 1. With numerous scalar couplings experienced by each proton and the short spectral range of chemical shift dispersion, the ^1H spectra of both rings severely overlap. In an earlier study similar problems were encountered in the analyses of ^1H NMR spectra of 2-(6-fluoro-1*H*-benzo[*d*]imidazol-2-yl)aniline, (4-(4-fluorobenzoyloxy)phenyl)methanol, 2-(4-(3-fluorobenzoyloxy)phenyl)acetic acid, 2-(4-(4-fluorobenzoyloxy)phenyl)acetic acid, 4-(4-chlorophenoxy)aniline, and 4'-fluorobiphenyl-2-carbaldehyde.²⁸ It was impossible to assign chemical shifts for individual protons especially in the aromatic regions and to determine all the associated coupling constants.

The two-dimensional COSY spectrum generally employed for the identification of coupled partners is shown in Figure 2 for compound **1** as an example. Though the COSY spectrum identifies the coupled partners, it does not discriminate the spin systems to aid the analyses. Therefore, the assignment of proton chemical shifts and the determination of coupling constants is a formidable task. Though other techniques such as soft-COSY, Z-COSY, etc. provide reduced multiplicity, the problem of overlap of the degenerate ^1H resonances from the two aromatic rings still persists. There are also reported pulse schemes for efficient excitation of multiple-quantum coherence in coupled networks of specified spin topology^{29,30} to aid the identification of spin systems. However, in such experiments the creation of multiple-quantum coherence is inhibited when the system departs from the specified spin topology. These pulse schemes can distinguish molecular fragments containing the same number of spins but different coupling patterns and are applicable to molecule **2**. However, the design and implementation of such sequences is not straightforward and also requires more than one experiment. Furthermore, when the spin topological network of protons is identical in both rings as in the present molecule **1**, the spin topological filtering cannot be applied. The fluorine-

* To whom correspondence should be addressed. E-mail: nsp@sif.iisc.ernet.in. Phone: ++91 80 22933300.

[†] Solid State and Structural Chemistry Unit.

[‡] NMR Research Centre.

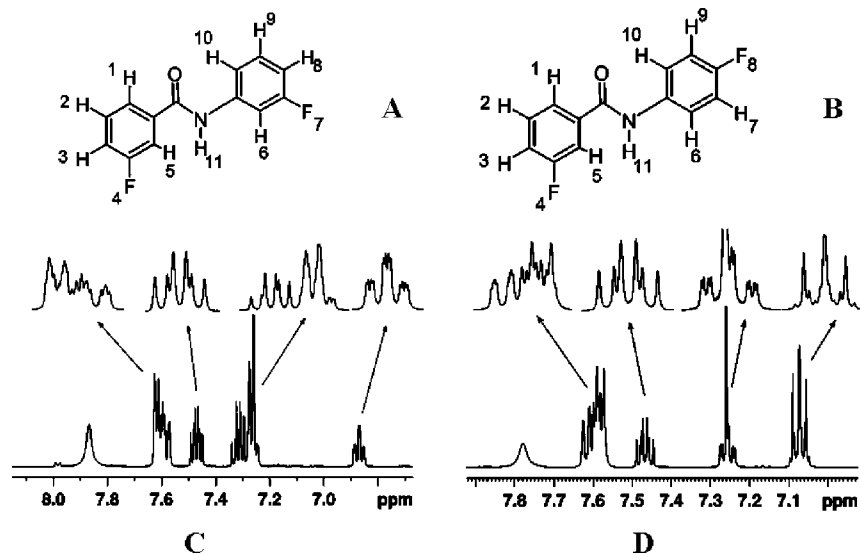


Figure 1. (A, B) Structures and numbering of interacting spins in 3-fluoro-*N*-(3-fluorophenyl)benzamide and 3-fluoro-*N*-(4-fluorophenyl)benzamide, respectively. (C, D) ^1H NMR spectra (500 MHz) of the compounds in (A) and (B), respectively, in the solvent CDCl_3 . The expansions of the crowded regions are depicted by arrows.

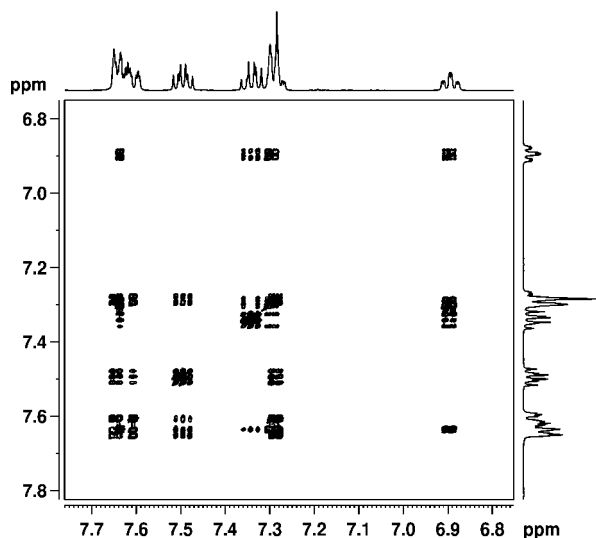


Figure 2. ^1H COSY (500 MHz) spectra of **1** along with F_1 and F_2 projections. The COSY experiment is well-known, and hence, the experimental details are not given.

decoupled one-dimensional ^1H spectrum also displays overlap of the spectra from two phenyl rings. In the present study we demonstrate the simplification of the analysis of such ^1H spectra by the application of two-dimensional multiple-quantum techniques with the incorporation of spin-state selection.

The coupling of the NH proton with the remaining protons and fluorines is undetectable. Consequently, each molecule **1** and **2** can be construed as two independent five-spin systems (four protons and one ^{19}F). The scalar couplings between the nearest inter-ring protons is also not detectable. This indicates that the simultaneous nonselective excitation of two possibilities of fourth-quantum (4Q) coherence of protons is feasible. The 4Q evolves at the cumulative additive values of four ^1H chemical shifts, which are different for each ring, so the two independent phenyl ring spectra, therefore, get separated in the 4Q dimension and by correlation should appear in different cross sections in the SQ dimension. Nevertheless, the complexity of the spectrum from each phenyl ring persists due to overlap of two subspectra corresponding to the $|\alpha\rangle$ and $|\beta\rangle$ spin states of ^{19}F . These two subspectra can also be separated from each other using spin-

state selection by the passive ^{19}F spin. Thus, all the proton transitions from the ^1H one-dimensional spectrum can be separated into four subspectra, each containing 1/4 the number of transitions from which assignment of the chemical shifts and extraction of the homonuclear coupling constants are significantly simplified. When either of the two proton resonances from any ring is distinctly identifiable and does not overlap with any proton resonances from the other ring, the spin-selective double-quantum (DQ)–SQ resolved experiment²⁷ can be employed to derive remote couplings of smaller magnitudes.

2. Experimental Section

The two isomers of difluorinated benzamides, molecules **1** and **2** with the substitution of fluorine in each phenyl ring, were prepared by the method described in the literature.³¹ The isotropic solutions of the molecules were prepared in the solvent CDCl_3 . All the spectra were recorded using a Bruker DRX-500 NMR spectrometer. The molecular structures with the numbering of the interacting spins and their corresponding one-dimensional ^1H spectra are given in Figure 1. The proton 4Q–SQ correlation experiments were carried out on both molecules using the multiple-quantum pulse sequence reported in Figure 3A. The delay, τ , required for creating the homonuclear antiphase magnetization during the evolution period was optimized for each molecule. The two-dimensional 4Q–SQ correlation spectra of the molecules are given in Figure 4 along with the corresponding F_1 and F_2 projections. Expansions of the selected regions of the spectra and the cross sections for **1** are reported in Figure 5. For the determination of remote couplings of smaller magnitudes, our recently developed spin-selective double-quantum (SSDQ) *J*-resolved pulse sequence,²⁷ shown in Figure 3B, has been employed. The SSDQ *J*-resolved spectra of the selectively excited spins for molecule **1** are reported in Figure 6. All the acquisition and processing parameters are reported in the corresponding figure captions.

3. Results and Discussion

The one-dimensional ^1H NMR spectrum of each molecule pertains to 11 interacting spins. In both molecules the NH proton does not exhibit any measurable coupling to the remaining protons. Consequently, the complex proton spectrum of the

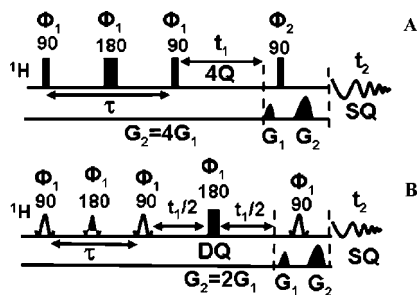


Figure 3. (A) Pulse sequence used for the multiple-quantum 2D experiments with nonselective excitation of homonuclear 4Q. The delay $\tau/2$ was optimized for the selection of proton homonuclear 4Q for both molecules. The gradient ratio was set to 1:4. In heteronuclear spin systems the sequence mimics the spin-selective pulse sequence used for the homonuclear spin system. The phase cycling is $\Phi_1 = \Phi_2 = \Phi_R = 0$. (B) Pulse sequence for the spin-state-selective SSDQ J -resolved experiments. The sequence is identical to that in (A) except the 180° pulse in the middle of the t_1 period is nonselective for protons. The phase cycling is $\Phi_1 = \Phi_R = 0$. Other details are discussed in the text.

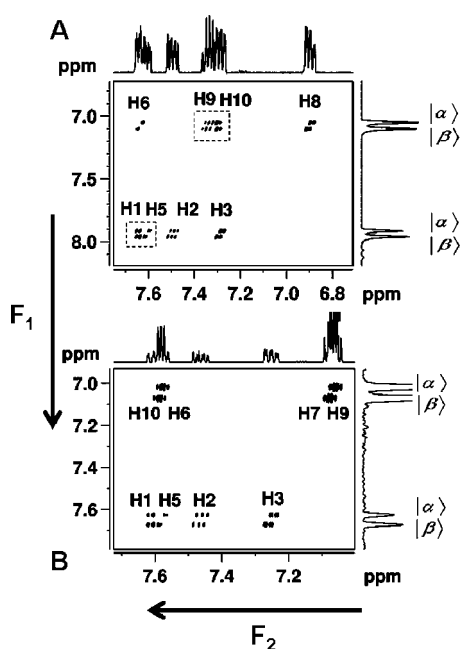


Figure 4. (A) ^1H 4Q–SQ correlation (500 MHz) spectra of **1** along with the F_1 and F_2 projections. The size of the 2D data matrix is 1740×720 and zero filled to 2048×1024 data points. The optimized τ delay is 41.67 ms. The time domain data were processed with the sine bell window function in both dimensions. The digital resolution in the F_1 and F_2 dimensions is 1.17 and 0.4 Hz, respectively. The four transitions in the 4Q dimension pertain to two spin states of ^{19}F of each phenyl ring marked $|\alpha\rangle$ and $|\beta\rangle$, respectively. The assignments of the chemical shifts for different protons are also marked. (B) ^1H 4Q–SQ correlation (500 MHz) spectra of **2** along with the F_1 and F_2 projections. The size of the 2D data matrix is 2100×700 . The optimized τ delay is 33.33 ms. The data were zero filled to 4096×1024 points before processing. The sine bell window function was used in both dimensions for processing. The digital resolution in the F_1 and F_2 dimensions is 0.49 and 0.12 Hz, respectively. The four transitions in the 4Q dimension pertain to two spin states of ^{19}F of each phenyl ring. The assignment of the chemical shift for protons is given.

molecule pertains to the ten interacting spins with eight protons and two fluorines. The 1D ^1H spectrum does not display eight distinct chemical shifts. Overlap of many ^1H resonances from the two phenyl rings is obvious. For the unambiguous analyses of the spectrum, the unraveling of the overlapped transitions is a prerequisite. Being separated by seven bonds, the coupling

between inter-ring spins is undetectable, and hence, the spectrum of each molecule can be construed as an overlap of two independent five-spin spectra. The highest homonuclear multiple-quantum excitation possible in each of the two independent five-spin systems is a fourth quantum of protons. In **1**, the coupled protons and fluorine of each phenyl ring of this molecule pertain to the weakly coupled spin systems of the type AFKPX, where X is the ^{19}F spin and the remaining spins are protons. The ^1H -detected spectrum is the AFKP part of this AFKPX spin system. In **2**, the spin topologies of the two rings are different and the spin systems are of the types AA'MM'X and AFKPX for the phenyl rings with fluorine substitution in the para and meta positions, respectively.

The simultaneous excitation of all the coupled protons using the pulse scheme in Figure 3A leads to the spin-selective excitation of 4Q of a five-spin system. This is a situation where all the coupled protons are active spins and ^{19}F is a passive spin. In the 4Q dimension the protons evolve only under the sum of passive (heteronuclear) couplings and at the cumulative additive values of the proton chemical shifts. Although many proton resonances from the two rings are degenerate, there are proton resonance(s) which are nondegenerate. Thus, the sum of four chemical shifts is different for the two rings. This difference in the cumulative additive values of the chemical shifts of ^1H 's between the two phenyl rings being of measurable magnitude, the complete separation of two five-spin spectra is achieved in the 4Q dimension irrespective of their spin topologies. Thus, the two-dimensional multiple-quantum technique has been employed for filtering of the spectra in both molecules. However, the spectrum from each phenyl ring is still complex as each proton experiences three homonuclear couplings and one heteronuclear coupling. Furthermore, the ^1H spectrum in each ring is an overlap of two subspectra because of the $|\alpha\rangle$ and $|\beta\rangle$ spin states of ^{19}F and can be separated from each other using spin-state selection by ^{19}F .

3.1. Analysis of 4Q–SQ Correlated Spectra. With the simultaneous flipping of all the coupled protons, the five-spin system of the types AFKPX or AA'MM'X behaves like an AX spin system in the 4Q dimension, where A (all four coupled protons) is the superspin and X (fluorine) is the spectator spin. The 4Q dimension pertains to the detection of the A part of this AX spin system. Thus, each phenyl ring provides a doublet in the 4Q dimension centered at the cumulative additive values of their respective proton chemical shifts, with the doublet separation corresponding to the sum of all the heteronuclear couplings. The MQ–SQ conversion pulse does not interact with the spin states of ^{19}F . In such a correlation the 4Q coherence corresponding to the $|\alpha\rangle$ spin state of ^{19}F is correlated to SQ coherences corresponding to the $|\alpha\rangle$ spin state of ^{19}F , and there is no coherence transfer to the $|\beta\rangle$ domain SQ coherences.²⁷ The same analogy holds good for $|\beta\rangle$ domain MQ coherence. A complex multiplet which is difficult to analyze from the one-dimensional proton spectrum can be separated into individual subspectra in different cross sections depending on the passive spin states, thereby achieving spectral simplification. The cross section taken parallel to the single-quantum dimension at any of the spin states of ^{19}F , for each phenyl ring, contains a reduced number of transitions that are sufficient for the determination of the scalar couplings among the protons of that particular phenyl ring. The displacements of the subspectra corresponding to the $|\alpha\rangle$ and $|\beta\rangle$ spin states of ^{19}F at each chemical shift position of ^1H provide the heteronuclear couplings. The direction of tilt of these displacements differs depending on the relative signs of the heteronuclear couplings.

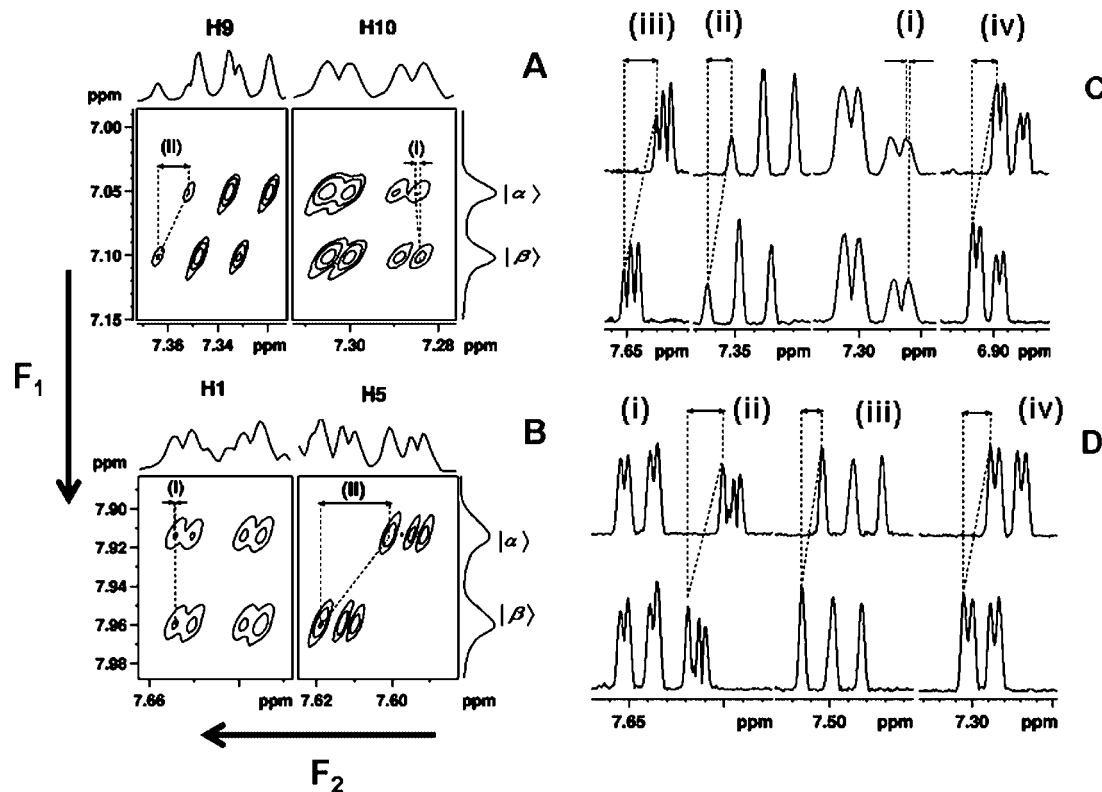


Figure 5. (A, B) Expansion of regions marked with broken rectangles in Figure 4A. (A) corresponds to the expanded region for the protons numbered 9 and 10, and (B) corresponds to the expanded region for the protons numbered 1 and 5. The opposite direction of tilt in (I) and (II) in (A) indicates the relative signs of these two J_{HF} values are opposite. This is true even in (B), but due to negligibly small couplings the opposite direction of tilt is not clearly evident. (C) Cross sections taken parallel to the F_2 dimension corresponding to spin states $|\alpha\rangle$ and $|\beta\rangle$ of ^{19}F of phenyl rings where the displacements of cross sections for peaks i, ii, iii, and iv are for the spins numbered 10, 9, 6, and 8, respectively. (D) Cross sections taken parallel to the F_2 dimension corresponding to spin states $|\alpha\rangle$ and $|\beta\rangle$ of ^{19}F of phenyl rings for the spins numbered 1, 2, 3, and 5. The marked directions of displacements i, ii, iii, and iv correspond to protons 1, 5, 2, and 3, respectively.

The 4Q–SQ correlation spectrum of **1** shown in Figure 4A clearly identifies the subspectra from the two phenyl rings. The difference in the cumulative additive values of all the proton chemical shifts $[(\text{H}_6 + \text{H}_9 + \text{H}_{10} + \text{H}_8) - (\text{H}_1 + \text{H}_5 + \text{H}_2 + \text{H}_3)]$ between the phenyl rings is 0.87 ppm, and the corresponding value in the 4Q dimension is 0.87 ppm. In the indirect dimension, the doublet centered at 7.94 ppm is assigned to the phenyl ring which has spins numbered 1–5, and the other doublet centered at 7.07 ppm is assigned to the phenyl ring which has spins numbered 6–10. Assignments to individual protons are significantly simplified after separation of the two independent five-spin spectra and are marked in the figure. The cross section taken parallel to the F_2 dimension in each phenyl ring position for either the $|\alpha\rangle$ or the $|\beta\rangle$ state of ^{19}F provides all the proton–proton couplings corresponding to the particular phenyl ring. The simplification of the spectral complexity is clearly evident from the subspectrum of each cross section, which contains only one-fourth the number of transitions encountered in the one-dimensional ^1H spectrum. The assignment of peaks to the individual protons of the phenyl rings is straightforward, and from the multiplicity pattern many homonuclear couplings could be determined and are reported in Table 1. The magnitude of the displacement of the subspectra between the cross sections and the inspection of the tilt direction at the chemical shift position of each proton pertaining to the $|\alpha\rangle$ and $|\beta\rangle$ states provided J_{HF} and its sign relative to that of the other J_{HF} values. It is clearly evident that three of the heteronuclear couplings (J_{HF}) have their displacement vectors tilted in the same direction and the tilt of one of the displacement vectors is opposite these three. This is obvious from the expanded regions

of spectra A and B of Figure 4, reported in Figure 5. The cross sections for the $|\alpha\rangle$ and $|\beta\rangle$ states of ^{19}F plotted under identical scales with the displacement vectors clearly identify the signs of the heteronuclear couplings. Furthermore, the algebraic sum of all J_{HF} values with appropriate sign combination is identical to the doublet separation in the 4Q dimension, confirming the relative signs of J_{HF} thus determined.

The 4Q–SQ correlation spectrum of **2** is given in Figure 4B along with the corresponding F_1 and F_2 projections. The difference in the cumulative additive values of all the proton chemical shifts between the phenyl rings is 0.61 ppm, which confirms the corresponding separation in the 4Q dimension. Thus, the distinctly different peaks for both phenyl rings could be filtered out in this molecule also. However, the first-order analysis of the spectrum corresponding to the phenyl ring with fluorine in the meta position is carried out similarly to that of the previous molecule. The displacement vector aided the determination of the coupling constant on the order of 0.03 Hz (experimental), which is hidden within the natural line width in the one-dimensional spectrum. However, the protons of the phenyl ring with fluorine in the para position form “nearly” an AA'XX' spin system due to accidental equivalence, and the first-order analysis of the spectrum of this strongly coupled spin system is not possible. Furthermore, the cross section taken along the SQ dimension at any of the spin states of ^{19}F in the 4Q dimension provided a deceptively simple spectrum with only four transitions of significant intensities. The iterative analysis of the spectrum for the extraction of all the coupling information with very few detectable weak transitions is tedious. Although heteronuclear couplings with the relative signs are determined

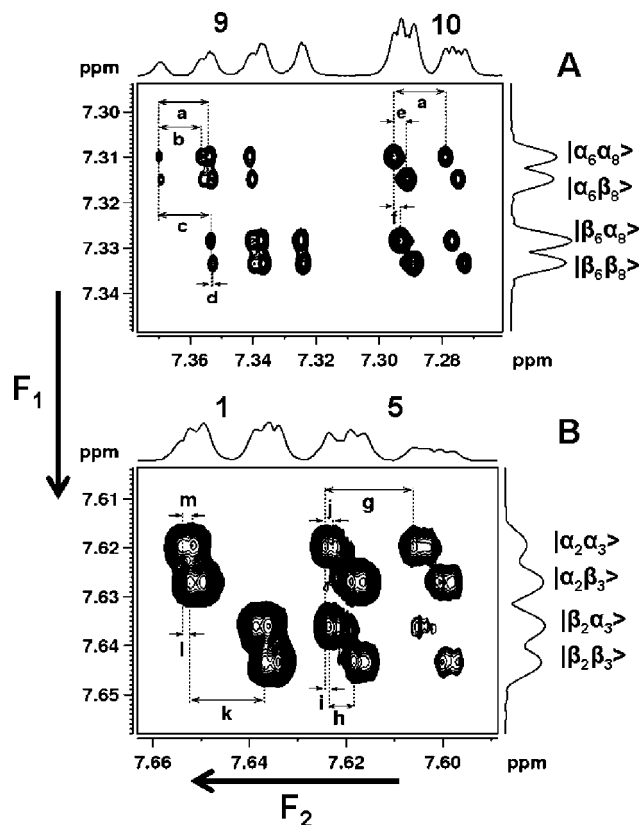


Figure 6. SSDQ J -resolved spectra of **1** in the isotropic solvent CDCl_3 . (A) Spectrum corresponding to the selective double-quantum excitation of protons 9 and 10. The size of the 2D data matrix is 512×96 . The optimized τ delay is 2.08 ms. The data were zero filled to 2048×1024 points before processing. The sine bell window function was used in both dimensions for processing. The digital resolution in the F_1 and F_2 dimensions is 0.07 and 0.06 Hz, respectively. The displacements providing the coupling information are (a) $J_{9,10}$, (b) J_{79} , (c) J_{89} , (d) J_{69} , (e) $J_{8,10}$, and (f) $J_{6,10}$. The marked spin states in the DQ dimension correspond to passive spins 6 and 8. (B) Spectrum corresponding to the selective excitation of protons 1 and 5. The size of the 2D data matrix is 512×48 . The optimized τ delay is 50.0 ms. The data were zero filled to 4096×1024 points before processing. The sine bell window function was used in both dimensions for processing. The digital resolution in the F_1 and F_2 dimensions is 0.04 and 0.03 Hz, respectively. The marked spin states in the DQ dimension correspond to passive spins 2 and 3. The displacements providing the coupling information are (g) J_{45} , (h) J_{35} , (i) J_{25} , (j) J_{15} , (k) J_{12} , (l) J_{13} , and (m) J_{15} . Notice the advantage of the experiment in measuring the precise values of the smaller couplings (J_{13} , J_{25} , J_{69} , and $J_{6,10}$) which are difficult to measure from the other experiments.

precisely for this ring, three of the homonuclear couplings could only be estimated. The determined spectral parameters are reported in Table 1 for this molecule also.

3.2. SSDQ J -Resolved Experiment. From Table 1 it is obvious that the magnitudes of the long-range homonuclear couplings, viz., ${}^5J_{\text{HH}}$, are very small and their extraction is severely hindered. These small couplings are hidden within the natural line width. For example, from Figure 5A at the chemical shift position of 9, a triplet pattern is observed. The topology of the spin system suggests that ${}^3J_{89}$ and ${}^3J_{9,10}$ are of comparable magnitudes and can account for this triplet. However, the ${}^5J_{69}$ coupling, being very small in magnitude compared to the natural line width, is undetectable. Thus, very small remote ${}^1\text{H}$ – ${}^1\text{H}$ couplings cannot be detected from the subspectrum of the 4Q–SQ correlation experiment.

Homonuclear spin-state selection by very small remote passive couplings, such as ${}^5J_{69}$, can be used to circumvent this

problem. For this to be achieved, the coupling to this remote proton must be retained in both dimensions and its spin state must not be disturbed during MQ–SQ conversion. Thus, this remote proton must be a passive spin throughout the correlation like a heteronucleus. This necessitates the application of a spin-selective pulse. Moreover, to avoid spin-state selection by the ${}^{19}\text{F}$ spin, a nonselective refocusing pulse on the protons in the middle of the MQ dimension has been applied which mimics ${}^{19}\text{F}$ decoupling. However, ${}^{19}\text{F}$ – ${}^1\text{H}$ coupling together with active coupling is present in the direct dimension. Hence, the spin-state-selective homonuclear DQ J -resolved sequence²⁷ has been applied, which retains coupling to remote passive proton spins in both dimensions and thereby achieves spin-state selection. Though small in magnitude compared to the line width, these remote passive couplings are now responsible for the relative displacements and are measurable. The pulse sequence for such an experiment is given in Figure 3B.

The two independent SSDQ J -resolved experiments have been performed on molecule **1**. Figure 6A corresponds to the spin-selective DQ–SQ correlation of protons 9 and 10 and with the application of a nonselective 180° pulse on protons in the middle of the t_1 dimension. In the DQ dimension the pulse sequence retains only the sum of passive couplings to protons 6 and 8 (i.e., $J_{69} + J_{6,10}$ and $J_{89} + J_{8,10}$), while the couplings to the fluorine spin are completely refocused. In such a situation the remaining two passive protons (6 and 8) of the corresponding phenyl ring mimic the heteronuclei. Each of the protons 6 and 8 has spin states $|\alpha\rangle$ and $|\beta\rangle$ and in the spin product basis has four eigenstates, $|\alpha_6\alpha_8\rangle$, $|\alpha_6\beta_8\rangle$, $|\beta_6\alpha_8\rangle$, and $|\beta_6\beta_8\rangle$, where the subscripts refer to protons 6 and 8. The spin states of the passive protons are not disturbed as the DQ–SQ conversion pulse is applied only on protons 9 and 10, providing spin-state selection. Thus, the DQ dimension will have four transitions, with the large doublet separation providing $J_{89} + J_{8,10}$, while the smaller doublet separation provides $J_{69} + J_{6,10}$. The separation in the DQ dimension would be identical to the chemical shift positions of both active spins. In the SQ dimension there are two displacement vectors for each of the spins 9 and 10 which provide both active and passive couplings. The two displacements at the chemical shift position of proton 9 can be utilized to determine individual values of J_{89} and J_{69} as reported in Figure 6A. The displacements at the chemical shift position of proton 10 can be exploited to derive individual values of $J_{8,10}$ and $J_{6,10}$. Thus, from this experiment the couplings, which were difficult to extract from the 4Q–SQ experiment, could be determined more precisely. The technique also overcomes the problem of field inhomogeneity contributions due to the 180° pulse in the middle of the t_1 dimension. A similar SSDQ J -resolved experiment was also carried out for the other ring of the molecule where the protons numbered 1 and 5 were selectively excited for double-quantum detection. This spectrum is reported in Figure 6B. The analysis of this spectrum was carried out similarly to that of Figure 6A. In this spectrum, also the displacements at the chemical shift position of proton 1 provided the individual couplings J_{12} and J_{13} and the displacements at the chemical shift position of proton 5 provided J_{25} and J_{35} .

The SSDQ J -resolved experiment was employed for the determination of long-range couplings in molecule **2** also. Although the protons of the meta ring are well isolated, the selective excitation of protons 1 and 5 is impossible without disturbance of protons 6 and 10 of the para ring. However, the bisselective excitation of protons 2 and 3 could be employed. This spectrum is not shown, but only the determined parameters

TABLE 1: Chemical Shifts and Couplings Determined for Molecules 1 and 2 in the Solvent CDCl_3 by Using 4Q–SQ Correlation and SSDQ J -Resolved Experiments^a

molecule 1		molecule 2		molecule 1		molecule 2	
parameter	value (δ , ppm; J , Hz)	parameter	value (δ , ppm; J , Hz)	parameter	value (δ , ppm; J , Hz)	parameter	value (δ , ppm; J , Hz)
δ_1	7.65 (7.65)	δ_6	7.64 (7.64)	δ_1	7.61 (7.61)	δ_6	7.58
δ_2	7.50 (7.48)	δ_7		δ_2	7.45 (7.46)	δ_7	7.06
δ_3	7.29 (7.29)	δ_8	6.90 (6.90)	δ_3	7.25 (7.25)	δ_8	
δ_4		δ_9	7.34 (7.34)	δ_4		δ_9	7.06
δ_5	7.61 (7.61)	δ_{10}	7.30 (7.29)	δ_5	7.58 (7.58)	δ_{10}	7.58
J_{12}	7.77 (7.73)	J_{67}	10.58 (10.61)	J_{12}	7.47 (7.46)	J_{67}^b	10.34
J_{13}	0.91 (0.61)	J_{68}	2.49 (2.27)	J_{13}	0.62 (0.42)	J_{68}	4.81
J_{14}	-0.35 (-0.31)	J_{69}	0.29 (0.10)	J_{14}	-0.03 (-0.11)	J_{69}	
J_{15}	1.38 (1.64)	$J_{6,10}$	2.12 (2.16)	J_{15}	1.53 (1.39)	$J_{6,10}^b$	5.81
J_{23}	8.37 (8.29)	J_{78}	8.49 (8.32)	J_{23}	8.29 (8.49)	J_{78}	8.21
J_{24}	5.61 (5.83)	J_{79}	6.5 (6.23)	J_{24}	5.55 (5.50)	J_{79}^b	5.81
J_{25}	0.41 (0.18)	$J_{7,10}$	-0.21 (-0.03)	J_{25}	0.64 (0.48)	$J_{7,10}$	
J_{34}	8.25 (7.90)	J_{89}	8.22 (8.25)	J_{34}	8.06 (7.81)	J_{89}	8.21
J_{35}	2.65 (2.66)	$J_{8,10}$	2.10 (2.14)	J_{35}	2.74 (2.74)	$J_{8,10}$	4.81
J_{45}	9.32 (9.42)	$J_{9,10}$	8.12 (8.01)	J_{45}	9.26 (9.27)	$J_{9,10}^b$	10.34

^a Errors of the parameters are on the order of digital resolution, whose values are reported in the figure captions. Values in parentheses are obtained by numerical iterations. ^b Values were estimated from the deceptively simple spectrum and are not precise.

are reported. As far as the phenyl ring with fluorine in the para position is concerned, the selective excitation of protons 6 and 10 is not possible due to severe overlap of transitions from the other ring. Nevertheless, protons 7 and 9 could be selectively excited. The cross section taken along the SQ dimension of this spectrum provides the active coupling J_{79} . The determined spectral parameters for both molecules are reported in Table 1. It is observed that in both molecules $^5J_{\text{HF}}$ (with the proton in the position para to the fluorine) is negative. Thus, two J_{HF} values are negative in **1**, and one J_{HF} value is negative in **2**.

Thus, the present study has several advantages; viz., it (a) filters the subspectra for different phenyl rings, (b) reduces the redundancy in the single-quantum transitions by spin-state selection of ^{19}F , simplifying the complexity of the spectrum by a factor of 4, and (c) provides both the magnitudes and relative signs of the heteronuclear couplings directly from the displacements without analysis of the 1D ^1H spectra. All these advantages enabled the spectral analyses of both molecules.

The precision of the determination of the spectral parameters has been further confirmed by the numerical iterative analyses of both cross sections along the SQ dimension corresponding to the $|\alpha\rangle$ and $|\beta\rangle$ spin states of ^{19}F for each phenyl ring. The computer program LEQUOR³² was employed. The chemical shifts and coupling constants obtained by the MQ–SQ correlation experiments were used as the starting parameters and were iterated further. All the chemical shifts and indirect couplings were independently varied during iteration. In **1**, for the phenyl ring with spins labeled 1–5, all 30 experimentally detected transitions were assigned to the root-mean-square error of 0.03 Hz, with no line deviating by more than 0.03 Hz. Similarly for the phenyl ring with spins labeled 6–10, 28 transitions were assigned to the root-mean-square error of 0.04 Hz. In **2**, as discussed previously the determination of the couplings for the phenyl ring with fluorine substitution in the para position was difficult due to very few detected transitions. However, for the ring with fluorine in the meta position, 30 lines were assigned to the root-mean-square error of 0.07 Hz. All the determined parameters obtained by the iterative analyses have been reported in Table 1. It is clearly evident from Table 1 that the experimentally measured values of the couplings are in close agreement with the numerically calculated values within the acceptable errors (digital resolution).

The aim of the present work is to demonstrate the simplification of the analyses of complex ^1H spectra with many interacting

spins. Further work in this direction on other isomers of benzamides with mono- and disubstituted fluorine and different halogens is in progress.

4. Conclusions

The one-dimensional proton spectra of isomers of difluorinated benzamides are very complex with many degenerate multiplet patterns. The present study exploits the difference between the cumulative additive values of proton chemical shifts of each phenyl ring for their separation using the nonselective excitation of homonuclear fourth-quantum coherence. This spin system filtering combined with spin-state-selective detection of the single-quantum transition significantly simplified the analyses of ^1H spectra as far as the determination of homonuclear couplings is concerned. The magnitudes of the displacements and the directions of the tilt of the displacement vectors at the chemical positions of each proton provide heteronuclear couplings and their relative signs. The spin-selective double-quantum J -resolved experiment aided the determination of remote couplings. $^5J_{\text{HF}}$ has been observed to be negative in both molecules.

Acknowledgment. N.S. gratefully acknowledges the Department of Science and Technology, New Delhi, for financial support (Grant No. SR/S1/PC-13/2004), and U.R.P. and B.B. thank CSIR, India, for a fellowship.

References and Notes

- (1) Günther, H. *NMR Spectroscopy, Basic Principles, Concepts, and Applications in Chemistry*; John Wiley & Sons: New York, 1992.
- (2) Ernst, R. R.; Bodenhausen, G.; Wokaun, A. *Principles of Nuclear Magnetic Resonance in One and Two Dimensions*; Clarendon Press: Oxford, U.K., 1991.
- (3) Keeler, J. *Understanding NMR Spectroscopy*; John Wiley & Sons: Chichester, England, 2005.
- (4) Jeener, J. Ampere Summer School, Basko Polje, Yugoslavia, 1971.
- (5) Aue, W. S.; Bartholdi, E.; Ernst, R. R. *J. Chem. Phys.* **1976**, *64*, 2229–2246.
- (6) Bachmann, S.; Aue, W. P.; Müller, L.; Ernst, R. R. *J. Magn. Reson.* **1977**, *28*, 29–39.
- (7) Nagayama, K.; Bachmann, P.; Wüthrich, K.; Ernst, R. R. *J. Magn. Reson.* **1978**, *31*, 133–148.
- (8) Macura, S.; Brown, L. R. *J. Magn. Reson.* **1983**, *53*, 529–535.
- (9) Shaka, A. J.; Keeler, J.; Freeman, R. *J. Magn. Reson.* **1984**, *56*, 294–313.
- (10) Neuhaus, D.; Wagner, G.; Vařák, M.; Käegi, J. H. R.; Wüthrich, K. *Eur. J. Biochem.* **1985**, *151*, 257–273.

- (11) Kay, L. E.; Bax, A. *J. Magn. Reson.* **1990**, *86*, 110–126.
- (12) Heikkinen, S.; Aitio, H.; Permi, P.; Folmer, R.; Lappalainen, K.; Kilpeläinen, I. *J. Magn. Reson.* **1999**, *137*, 243–246.
- (13) Bax, A.; Max, D.; Zax, D. *J. Am. Chem. Soc.* **1992**, *114*, 6923–6925.
- (14) Reif, B.; Köck, M.; Kerssebaum, R.; Schleucher, J.; Griesinger, C. *J. Magn. Reson., B* **1996**, *112*, 295–301.
- (15) Hu, J. S.; Bax, A. *J. Am. Chem. Soc.* **1997**, *119*, 6360–6368.
- (16) Oschkinat, H.; Pastore, A.; Pfändler, P.; Bodenhausen, G. *J. Magn. Reson.* **1986**, *69*, 559–566.
- (17) Brüschweiler, R.; Madsen, J. C.; Griesinger, C.; Sørensen, O. W.; Ernst, R. R. *J. Magn. Reson.* **1987**, *73*, 380–385.
- (18) Bax, A.; Freeman, R. *J. Magn. Reson.* **1981**, *44*, 542–561.
- (19) Griesinger, C.; Sørensen, O. W.; Ernst, R. R. *J. Chem. Phys.* **1986**, *85*, 6837–6852.
- (20) Pfändler, P.; Bodenhausen, G. *J. Magn. Reson.* **1987**, *72*, 475–492.
- (21) Montelione, G. T.; Winkler, M. E.; Rauenbuehler, P.; Wagner, G. *J. Magn. Reson.* **1989**, *82*, 198–204.
- (22) Sørensen, O. W. *J. Magn. Reson.* **1990**, *90*, 433–438.
- (23) Griesinger, C.; Sørensen, O. W.; Ernst, R. R. Two-dimensional correlation of connected NMR transitions. *J. Am. Chem. Soc.* **1985**, *107*, 6394–6396.
- (24) Eggenberger, U.; Karimi-Nejad, Y.; Thüning, H.; Rüterjans, H.; Griesinger, C. *J. Biomol. NMR* **1992**, *2*, 583–590.
- (25) Schmidt, J. M.; Ernst, R. R.; Aimoto, S.; Kainosho, M. *J. Biomol. NMR* **1995**, *6*, 95–105.
- (26) Bikash, B.; Suryaprakash, N. *J. Phys. Chem. A* **2007**, *111*, 5211–5217.
- (27) Bikash, B.; Suryaprakash, N. *J. Chem. Phys.* **2007**, *127*, 214510.
- (28) Caliendo, G.; Santagada, V.; Perissutti, E.; Severino, B.; Fiorino, F.; Warner, T. D.; Wallace, J. L.; Ifa, D. R.; Antunes, E.; Cirino, G.; de Nucci, G. *Eur. J. Med. Chem.* **2001**, *36*, 517–530.
- (29) Levitt, M. H.; Ernst, R. R. *Chem. Phys. Lett.* **1983**, *100*, 119–123.
- (30) Levitt, M. H.; Ernst, R. R. *J. Chem. Phys.* **1985**, *83*, 3297–3310.
- (31) Chopra, D.; Guru Row., T. N. *Cryst. Eng. Commun.* **2008**, *10*, 54–67.
- (32) Diehl, P.; Kellerhals, H. P.; Niederberger, W. *J. Magn. Reson.* **1971**, *4*, 352–357.

JP8055174